Enhancement of Quantum Dot Förster Resonance Energy Transfer within Paper Matrices and Application to Proteolytic Assays

Hyungki Kim, Eleonora Petryayeva, and W. Russ Algar

***Abstract*—Brightly luminescent semiconductor quantum dots (QDs) continue to have an increasing role in biophotonic research and applications such as bioassays. Here, we present methods for the immobilization of QDs on the cellulose fibers of paper substrates for Förster resonance energy transfer (FRET)-based assays of proteolytic activity. Steady-state and time-resolved fluorescence characterization of FRET between immobilized QDs and self-assembled dye-labeled peptides within the paper matrix revealed a substantial enhancement in energy transfer efficiency. Compared to bulk solution, the rate of energy transfer increased approximately 4-fold resulting in a concomitant 7-fold increase in the ratio of FRET-sensitized acceptor dye emission and quenched QD emission. Spots of immobilized QDs with different amounts of dye-labeled peptide had bright luminescence under UV/violet illumination and the net QD and A555 emission was visible by eye as different colors. Tryptic digestion of the peptide linking the QD donor and acceptor dye resulted in loss of FRET. Changes in the dye/QD PL ratio permitted tracking of proteolytic activity, including the effect of increasing amounts of aprotinin, a potent inhibitor of trypsin. The combination of QDs, a paper substrate, and enhanced FRET has strong potential for developing bioassays.**

***Index Terms*—Quantum dots, fluorescence, Förster resonance energy transfer (FRET), fluorescence lifetime imaging microscopy (FLIM), paper diagnostics, biosensors, proteases, inhibition assay.**

I. Introduction

THE unique optical and electronic properties of various nanoparticles (NPs) have been a major focus of biophotonic research in recent years. Materials as diverse as carbon allotropes [1, 2], noble metal NPs and nanoclusters [3, 4], lanthanide NPs [5], and semiconductor quantum dots (QDs) [6], among many others, have been used as optical probes for cellular imaging, theranostics, and *in vitro* assays and diagnostics. In each case, properties such as size, surface area, cargo capacity, and light absorption and emission have provided distinct functional advantages. For *in vitro* assays and diagnostics in particular, NPs can offer enhanced sensitivity [7-9], robustness, higher avidity and activity when functionalized with multiple biomolecular probes [10, 11], and greater capacity for multiplexing [12].

Although advances in the capabilities and availability of both NP materials and sophisticated optical technologies have led to the development of better bioassays, the accessibility and practicality of many of these approaches can be limited to advanced research and clinical laboratories. There is a significant need for simple, low-cost, portable, and robust bioassays that are suitable for lower resource settings such as field deployment, patient point-of-care, and use in developing countries. To address these needs, there has been a surge in research toward test strips, lateral flow assays, and micro-paper analytical devices (μPADs) [13-15]. Many recent efforts have sought to incorporate NPs and their associated advantages into these technologies. In particular, gold NPs have been extensively utilized [16], largely due to their facile synthesis, intense coloration, red-to-blue color change upon aggregation [9], and silver enhancement methods [17]. In comparison, low-cost assays with QDs have been much less investigated, albeit that a few lateral flow immunoassays [18-20] and paper-based assays [21, 22] have been reported. Here, we also investigate the potential for paper-based assays with QDs through both fundamental spectroscopic characterization and an example of a bioassay for proteolytic activity and inhibition. While not without potential challenges, paper-based assays with QDs are a promising avenue for research given the widely reported capabilities of QDs in other bioimaging and bioanalysis formats.

II. Quantum dots as FRET-Based Bioprobes

QDs have emerged as important labels for cellular, tissue, and single molecule imaging [12, 23, 24]. The principal advantages of QDs in these applications are their broad absorption spectra, large one-photon (10^4–10^7 M^{-1} cm^{-1}) and two-photon (10^3–10^4 GM) absorption coefficients, narrow and symmetric PL emission spectra (25–35 nm full-width-at-half-maximum, FWHM), the ability to tune the PL emission wavelength through nanocrystal size and composition, and resistance to photobleaching [6, 25]. These properties also offer superior performance and more straightforward implementation of multicolor imaging. QDs can be modified with antibodies or other affinity ligands to target various

The authors thank the Natural Sciences and Engineering Research Council of Canada (NSERC), the Peter Wall Institute for Advanced Studies (PWIAS), the Canada Foundation for Innovation (CFI), and the University of British Columbia for support of this research. H. Kim was supported by an NSERC undergraduate research award. E. Petryayeva was supported by an NSERC postgraduate fellowship. W.R. Algar is supported by a Canada Research Chair (Tier 2). We thank Cheryl Ng for assistance with some experiments.

All authors are with the Department of Chemistry, University of British Columbia, Vancouver, BC V6T 1Z1, Canada (algar@chem.ubc.ca).

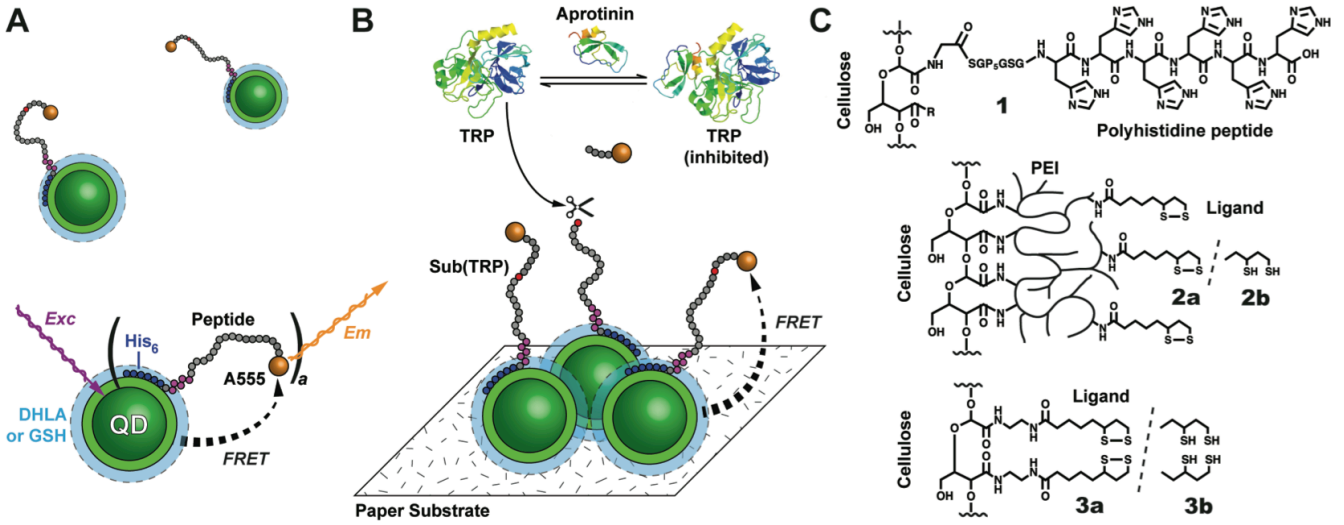

Fig. 1. (A) QDs self-assembled with hexahistidine (His_6) terminated A555-labeled peptides in bulk solution. Violet excitation of the QD (Exc) can result in FRET to the proximal A555 and sensitized emission (Em). (B) QD-peptide-A555 conjugates immobilized on a paper substrate. The peptide, Sub(TRP), can be cleaved by trypsin (TRP) at a specific site (see Table 1) resulting in loss of FRET and the ability to measure the inhibition of TRP by aprotinin. (C) Different ligands used to chemically modify the cellulose fibers of the paper to immobilize QDs via self-assembly. The PEI is drawn stylistically. Figure is not drawn to scale.

biomarkers, cells, and tissues.

Another prominent area of interest that benefits from the above properties of QDs is the development of Förster resonance energy transfer (FRET)-based probes where changes in PL intensity are used to signal the presence or activity of biological targets [26, 27]. The most common role of QDs in FRET systems is as donors. The narrow PL of the QD allows the spectral overlap with an acceptor chromophore to be maximized while also minimizing crosstalk when measuring both donor and acceptor emission. Moreover, the ability to excite QDs across a broad range of wavelengths allows direct excitation of acceptors to be minimized. The FRET efficiency can also be systematically enhanced by arraying multiple acceptors per QD. Various dark quenchers [28, 29], fluorescent dyes [29, 30], fluorescent proteins [7, 31, 32], and gold nanoparticles [33, 34] have been paired as acceptors with QD donors. Recent studies have further demonstrated energy transfer between QDs and carbon nanomaterials [35-37]. To a much lesser but nonetheless growing extent, QDs have also been utilized as acceptors for luminescent lanthanide complexes [38, 39], chemiluminescent species [40], and bioluminescent proteins [41].

QD-FRET probes have been developed for a multitude of different biological targets and operate through a variety of transduction mechanisms [26, 27]. One such mechanism is associative, where a biorecognition process generates the proximity needed for FRET. Examples have included sandwich immunoassays [42] and sandwich hybridization assays [8]. In contrast, a dissociative mechanism relies on a biorecognition process eliminating the proximity required for FRET, as demonstrated with hydrolytic enzymes such as proteases [29] and nucleases [43]. Competitive binding assays have been demonstrated with QDs and FRET for nutrients [44], DNA [45], and RNA [46], among other targets. Unlabeled endogenous target typically displaces dye-labeled exogenous target in these assays. As another transduction mechanism, changes in biomolecular conformation upon biorecognition are often utilized to modulate donor-acceptor distance and FRET efficiencies without complete dissociation. This format is epitomized by QD-based molecular beacons for DNA detection [47]. More recently, QD-FRET probes for detecting changes in biological environments have been developed on the basis of changes in spectral overlap between QD donors and dye acceptors, as demonstrated with pH sensing [48]. Detection of some analytes is also possible by altering acceptor re-emission rather than FRET efficiency. This type of format has been demonstrated for reagentless maltose sensing [49] and oxygen sensing [50].

In addition to the diverse targets already mentioned, energy transfer-based QD probes have recently been reported for glucose and galactose [51], cocaine [52], kinase and phosphatase activity [53, 54], fluoride [55], mercuric ion [56], renin [57], carcinoembryonic antigen [58], mucin 1 [59], and many other analytes too numerous to mention here. The vast majority of the above assays have had a homogeneous format (*i.e.* solution phase). Comparatively few heterogeneous (*i.e.* solid phase) FRET-based assays have been developed with QDs. The few examples have included protease assays on glass chips [34] and nucleic acid hybridization assays on optical fibers [60], within microtiter plate wells [61], or, most recently, on paper substrates [21].

In this study, we present and evaluate three different methods for the immobilization of QDs within a paper matrix, compare FRET between solution and paper environments, and demonstrate a paper-based protease inhibition assay. Alexa Fluor 555 (A555) labeled peptides are self-assembled to CdSeS/ZnS core/shell QDs in bulk solution (Fig. 1A) and within the paper matrix (Fig. 1B). For the latter, QDs are immobilized through self-assembly after chemically modifying the cellulose fibers of the paper with ligands (Fig. 1C) that have high affinity for the ZnS shell of the QDs. Within the paper matrix, substantial increases in the relative

amount of FRET-sensitized A555 emission and the FRET efficiency are observed using steady-state and fluorescence lifetime measurements. When the A555-labeled peptide sequences are designed to be a substrate for a protease such as trypsin (TRP), it is possible to detect proteolytic activity through changes in FRET and measure the effect of an increasing amount of a protease inhibitor such as aprotinin. Our results show that the combination of QDs, a paper matrix, and the concomitant enhancement in FRET is suitable for developing sensitive assays for proteolytic activity.

III. Materials and Methods

A. Preparation of Water Soluble Quantum Dots

Hydrophobic CdSeS/ZnS quantum dots with an emission maximum at 525 nm (Cytodiagnostics, Burlington, ON, Canada) were made water-soluble through ligand exchange with L-glutathione (GSH) or dihydrolipoic acid (DHLA) as described elsewhere [61].

B. Peptide Labeling

The peptide sequences in Table 1 (Biosynthesis Inc., Lewisville, TX) were labeled with Alexa Fluor 555 C2 maleimide (Life Technologies, Carlsbad, CA) at their C-terminal cysteine residue as described previously [62]. In experiments with unlabeled peptides, the cysteine residue was capped with pyridyl disulfide to avoid oxidative crosslinking between peptides or coordination of the cysteine to the surface of the QD. Unlabeled peptide (100 µL, 100 µM) in 50% acetonitrile with borate buffer (100 mM, pH 8.7, 50 mM NaCl) was mixed with a solution of Aldrithiol-2 (100 µL, 500 µM; Sigma-Aldrich) in the same solvent and let stand at room temperature overnight.

TABLE 1
PEPTIDE SEQUENCES

Name	Sequence (N-terminal to C-terminal)
Pep-A555	H_6SP_6SGQGEGEGNSAAYASGNGC-A555
Sub(TRP)-A555[a]	H_6SP_6SGQGEGEGNSG**R**GGSGNGC-A555

[a] The TRP cleavage site is highlighted in bold.

C. Chemical Modification of Paper Substrates

Whatman (Florham, NJ) no. 4 cellulose filter paper was incubated in 100 mM $NaIO_4$ (Sigma-Aldrich, Oakville, ON, Canada) for 1 h in the dark. The paper was washed three times with deionized water, rinsed once each with methanol and dichloromethane (DCM), then dried *in vacuo* for ≥ 6 h. One of three different derivatization protocols (i-iii) was utilized thereafter:

(i) To derivatize the oxidized paper substrates with **1** (see Fig. 1C), a 20 µL solution with 290 µM of the peptide sequence GSGPPPPPGSGHHHHHH (Biosynthesis Inc.) and 50 mM $NaCNBH_3$ was spotted onto the paper and incubated for 24 h in a humid chamber. The paper was then rinsed with borate buffer (25 mM, pH 8.7).

(ii) To derivatize oxidized paper with **2a** (see Fig. 1C), the paper was incubated in a solution of 50 mM $NaCNBH_3$ and 44 mM poly(ethyleneimine) (PEI; MW ~12 kDa, Sigma-Aldrich) in bicarbonate buffer (pH 9) for 1 h. The paper was then washed twice with deionized water, once with ~0.01 M HCl (aq), again with water, and once with ethanol. Next, the paper was treated with a 2 mL solution of 60 mM lipoic acid, 67 mM *N*-hydroxysuccinimide, and 69 mM *N*,*N*'-diisopropyl-carbodiimide (Sigma-Aldrich) in tetrahydrofuran (THF) for 24 h. The paper was then washed three times with THF, once with ethanol, and once with deionized water.

(iii) To derivatize oxidized paper with **3a** (see Fig. 1C), the paper was incubated in a *ca.* 20 mM solution of *N*-(2-aminoethyl)-5-(1,2-dithiolan-3-yl)pentanamide in DCM for ≥ 3 h, washed three times with DCM, incubated with 50 mM $NaCNBH_3$ (aq) for 1 h, and then washed three times with water, once with methanol, and once with DCM. The paper was dried *in vacuo* for ≥ 20 min and then stored at –20 °C.

The paper with **2a** or **3a** was reduced to **2b** and **3b**, respectively, with a 50 mM $NaBH_4$ solution for ≥ 2 h, then washed with water and ammonium acetate buffer (pH 4.5). The paper was dried *in vacuo* for 10–30 min.

D. Stepwise Immobilization of QDs and Peptides

DHLA- or GSH-QDs (2.8 µM) were spotted on paper modified with **3b** in two consecutive 0.5 µL increments and let stand for 1 h. Next, 4 µL of peptide solution (50 µM) was spotted on the spots of QDs and let stand for 1 h. Both incubation steps were done in a humid chamber. The paper substrates were then washed in borate buffer (25 mM, pH 8.7). Samples were kept hydrated prior to measurements.

E. Immobilization of Pre-Assembled QD-Peptide Conjugates

GSH-QD-peptide conjugates were pre-assembled by mixing QDs with the desired ratio of peptide in borate buffer (100 mM, pH 9.2) for 1 h. The final concentration of QDs was 2.8 µM. The conjugates were then spotted on paper modified with **3b** in two 0.5 µL increments then let stand for 1 h before washing with borate buffer (25 mM, pH 8.7).

F. PL Measurements

Absorption and PL emission spectra of QDs and QD-peptide conjugates in solution were obtained with an Infinite M1000 Pro multifunction plate reader (Tecan Ltd., Morrisville, NC, USA) using non-binding 96-well plates. Absorption and PL emission spectra of QDs and QD-peptide conjugates immobilized on paper substrates were also obtained using the Infinite M1000 Pro by sandwiching pieces of paper substrate between the windows of a NanoQuant plate (Tecan Ltd.). For PL emission measurements, an excitation wavelength of 400 nm was used. Excitation and emission bandwidths were both 5 nm.

FLIM was done with a Zeiss LSM510 scanning confocal microscope equipped with a time-correlated single-photon counting (TCSPC) fluorescence lifetime imaging module (Becker & Hickl GmbH, Berlin, Germany) and a tunable Chameleon XR femtosecond laser (Coherent, Santa Clara, CA) for two-photon excitation (840 nm). Data acquisition was done over 16 wavelength channels with an xy-resolution of 128 × 128 pixels and 256 time channels. QD PL was detected in the 525 nm channel.

For assays of proteolytic activity, PL measurements were

made using the simple setup shown in Fig. 2. A low-cost LED with emission at 405 nm (Visual Communications Company, VAOL-5GUV0T4, Poway, CA, USA) was used as the excitation source and simple optics were used to collect PL emission from QD-modified paper substrates. Scattered excitation light was rejected using a 450 nm longpass filter (Thor Labs, Newton, NJ, USA) and emission was coupled into a portable fiber-optic spectrometer (GreenWave 16 VIS-50, StellarNet, Tampa, FL, USA). Spectra were collected at regular intervals using a custom data acquisition program written in LabVIEW (National Instruments, Austin, TX, USA).

All PL measurements were made on paper samples hydrated with buffer.

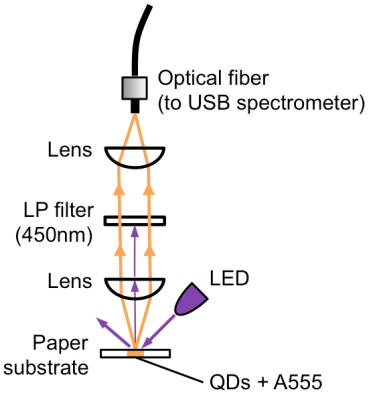

Fig. 2. Schematic of the optical setup used to measure QD and A555 PL from modified paper substrate during TRP inhibition assays. LP = long pass filter. LED = light emitting diode.

G. Analysis of FRET

A555/QD PL ratios, $\rho_{A/D}$, were calculated with (1), where $I(\lambda)$ is the PL intensity at wavelength λ, and $\sigma_{D,\lambda}$ (≈ 0.02 at 570 nm) is a correction factor accounting for the relative crosstalk of the QD emission at a wavelength with predominant A555 emission.

$$\rho_{A/D} = \frac{I(570\text{ nm}) - \sigma_{D,570\text{ nm}} I(525\text{ nm})}{I(525\text{ nm})} \tag{1}$$

FRET efficiencies, E, were measured from changes in QD PL intensity or lifetime relative to samples without any acceptor according to (2), where I is the PL intensity of a sample with acceptor, I_0 is the reference intensity (no acceptor), τ_{av} is the average lifetime of a sample with acceptor, and $\tau_{0,av}$ is the average reference lifetime.

$$E = 1 - (I/I_0) = 1 - (\tau_{av}/\tau_{0,av}) \tag{2}$$

The average lifetime used in (2) is the amplitude weighted lifetime (3) derived from fitting PL decay curves with a biexponential function (4) [63].

$$\tau_{av} = \frac{A_1\tau_1 + A_2\tau_2}{A_1 + A_2} \tag{3}$$

$$I(t) = A_1 e^{-t/\tau_1} + A_2 e^{-t/\tau_2} \tag{4}$$

FRET efficiencies were also estimated from the relative QD donor and A555 acceptor emission using (5), where $I_A(\lambda)$ and $I_D(\lambda)$ are the acceptor and donor emission intensities as a function of wavelength, and Φ_A and Φ_D are the respective quantum yields.

$$E = \frac{\int I_A(\lambda)d\lambda}{(\Phi_A/\Phi_D)\int I_D(\lambda)d\lambda + \int I_A(\lambda)d\lambda} \tag{5}$$

Plots of FRET efficiency versus number of acceptors per QD, a, were fit with (6), where R_0 is the Förster distance for the QD-acceptor dye pair and r is their center-to-center separation.

$$E = \frac{aR_0^6}{aR_0^6 + r^6} = \frac{a}{a + (r/R_0)^6} \tag{6}$$

The Förster distance was calculated from (7), where n (= 1.33) is the refractive index of the medium, κ^2 (= 0.67) is the orientation factor, Φ_D is the quantum yield of the QD donor, $I_D(\lambda)$ is the PL intensity of the QD donor at wavelength λ, and $\varepsilon_A(\lambda)$ is the molar absorption coefficient ($\text{cm}^2\ \text{mol}^{-1}$) of the acceptor at λ [63]. The integrals on the right-hand side represent the spectral overlap, J.

$$R_0^6 = (8.79\times10^{-28}\text{ mol})\, n^{-4}\kappa^2\Phi_D \frac{\int I_D(\lambda)\varepsilon_A(\lambda)\lambda^4 d\lambda}{\int I_D(\lambda)d\lambda} \tag{7}$$

FRET rates, k_{FRET}, were calculated from (8) after obtaining the value of $(R_0/r)^6$ from least-squares fitting of efficiency *versus* acceptors per QD curves and substituting $\tau_{0,av}$ from fluorescence lifetime measurements [63].

$$k_{FRET} = \tau_{0,av}^{-1}(R_0/r)^6 \tag{8}$$

H. Proteolytic Assays

Spots of QD-Sub(TRP)-A555 conjugates were immobilized on paper substrates as described above. A 100 µL solution of 2 µM trypsin (TRP; ≥10000 BAEE units/mg protein; EC number: 3.4.21.4) and 0–40 µM aprotinin in borate buffered saline (BBS; 10 mM, pH 8.7, 50 mM NaCl) was added to a spot of QD-Sub(TRP)-A555 and the PL spectrum was measured at 1 min intervals for 1 h under LED illumination (405 nm). The PL ratios were calculated from the measured spectra and, for each sample, normalized to the initial PL ratio. To account for any changes in QD brightness over the assays, each data set was then normalized to a negative control sample (0 µM TRP, 40 µM aprotinin) at all time points. The data was fit with an empirical function and the initial rate of substrate digestion estimated as the slope of the tangent at 1 min.

IV. Results and Discussion

A. Immobilization Methods

Three different strategies were investigated for the immobilization of water soluble QDs on the cellulose fibers of paper substrates. In control experiments, the fibers themselves were found to have no measurable affinity for QDs. As shown in Fig. 3, QD PL could not be detected after exposure of untreated paper to an 11 µM solution of DHLA-QDs with subsequent washing. To impart affinity, the fibers were modified with ligands that were able to tightly bind the QDs. In each case, the cellulose fibers were first activated by mild oxidation with sodium (meta)periodate [64] then reacted in one or more steps to generate pendant ligands. The details of

the chemistry are described in the Materials and Methods section and Fig. 1C shows the molecular structures.

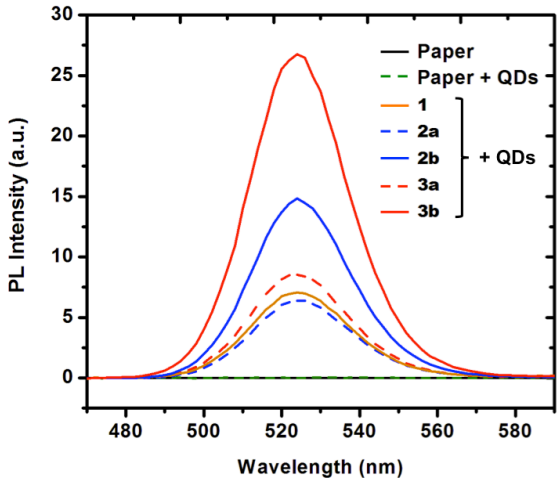

Fig. 3. Background corrected PL emission spectra of paper substrates after exposure to QDs with and without modification of their cellulose fibers with the affinity ligands shown in Fig. 1C.

The first ligand (**1**) that was tested for the immobilization of QDs on paper fibers was inspired by the widely reported success of conjugating polyhistidine-appended biomolecules to QDs. Medintz and coworkers have demonstrated that proteins [32, 44, 65-68], peptides [29, 68-71], and DNA [30, 47, 72] can be controllably self-assembled to QDs through dative interactions between the imidazole ring of histidine residues and the ZnS shell of QDs. Other groups have also utilized this methodology for bioconjugation of QDs [73-75], and planar glass surfaces modified with polyhistidine appended peptides have been shown to immobilize QDs [76]. In our experiments, we reacted oxidized paper fibers with the N-terminus of a short (17 residue) peptide with a C-terminal hexahistidine sequence. As indicated by the QD PL emission spectrum in Fig. 3, the peptide modified paper fibers were able to bind and immobilize DHLA-QDs.

The second (**2a/b**) and third (**3a/b**) methods that were tested for the immobilization of QDs made use of lipoic acid derivatives as pendant ligands on cellulose paper fibers. Similar to imidazole rings, thiol groups also have high affinity for the ZnS shell of QDs. Bifunctional thiolate molecules, such as DHLA, are widely used to modify the surface of QDs to provide aqueous solubility [77-79], and lipoic acid derivatives have been used to immobilize thin films of QDs on glass and fused silica substrates [80]. Here, activated paper fibers were either first reacted with branched PEI and then modified with lipoic acid (**2a/b**), or, alternatively, were directly reacted with a lipoic acid derivative (**3a/b**). The affinity of these modified paper substrates for QDs was tested both with and without reduction of the lipoic acid dithiolane group (**2a**, **3a**) to a dithiol group (**2b**, **3b**). In both cases, the dithiol form (**2b**, **3b**) had *ca.* 2–3-fold greater affinity than the dithiolane form (**2a**, **3a**). Fig. 3 shows an example of representative data. Overall, the immobilization method that produced the brightest spots of QDs was direct modification of paper with a lipoic acid derivative (**3b**). The brightness of the spots of QDs was determined by both the immobilization efficiency and the effect (if any) of immobilization on the quantum yield of the QDs, albeit that the former was expected to be the dominant factor. Spots of QDs immobilized using the peptide (**1**) and PEI-lipoic acid (**2a/b**) methods had < 30% and < 75%, respectively, of the brightness of spots prepared using direct modification with lipoic acid (**3b**). No significant differences in the peak emission wavelength or FWHM of the QDs was observed between the three immobilization methods. The superior brightness, simpler preparation (*cf.* PEI), and lower-cost reagents (*cf.* peptide) made the direct modification of cellulose fibers with lipoic acid the preferred method for QD immobilization on paper substrates. Therefore **3b** was used in all subsequent experiments.

B. The QD-A555 FRET Pair

The absorption and emission spectra for the QD and A555 labeled peptide are shown in Fig. 4 along with the qualitative spectral overlap. Table 2 summarizes important photophysical parameters. Note that GSH-coated QDs were used in all FRET experiments because they provided a 4-fold higher quantum yield than DHLA-coated QDs. The quantum yield of A555-labeled peptide was measured to be ~0.09.

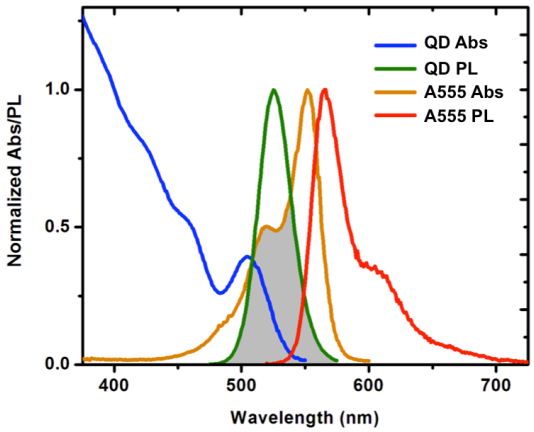

Fig. 4. Absorption (Abs) and PL spectra for the QD-A555 FRET pair. The qualitative spectral overlap is shaded. These spectra are also a useful reference for interpreting Fig. 5 and Fig. 7.

TABLE 2
PROPERTIES OF THE QD-A555 FRET PAIR

$\lambda_{em,D}$ [a] (nm)	Φ_D	$\lambda_{abs,A}$ [b] (nm)	$\varepsilon_{max,A}$ [c] (M^{-1} cm^{-1})	J [d] (cm^6 mol^{-1})	R_0 (nm)
525	0.20	554	150 000	6.4×10^{-10}	5.4

[a] Wavelength of maximum donor PL emission; [b] wavelength of maximum acceptor absorption; [c] peak molar absorption coefficient for acceptor; [d] spectral overlap integral

To serve as a point of comparison for studying FRET with QDs immobilized on paper fibers, QDs were first assembled with different ratios of Pep-A555 peptide (Table 1) in bulk solution (*ca.* 0, 4, 8, 12, 16, and 20 per QD). Assembly was through the high-affinity interaction between the QDs and the hexahistidine tag of the peptide. The number of peptides per QD was confirmed by measuring the absorption spectra of the conjugates (Fig. 5A) with knowledge of the relative molar

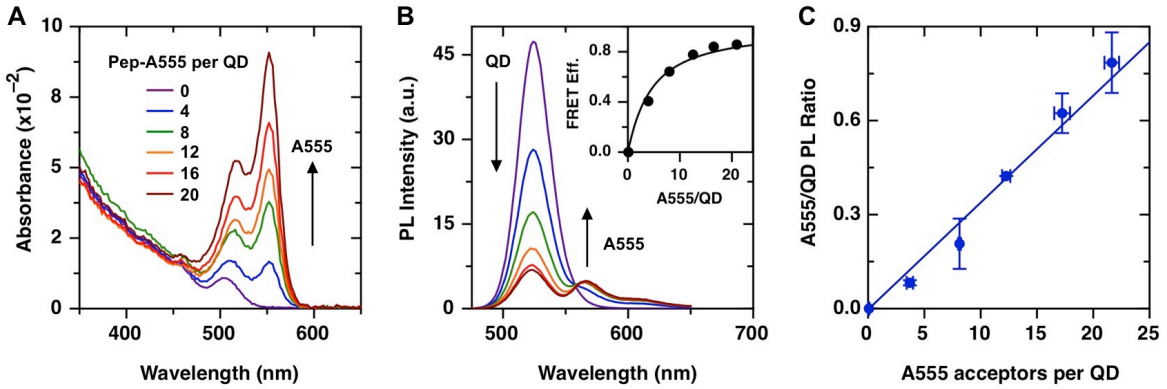

Fig. 5. Solution-phase FRET. (A) Representative absorption spectra showing the nominal assembly of ca. 0, 4, 8, 12, 16, and 20 per QD. The spectra are used to determine the actual number assembled. (B) PL emission spectra corresponding to the samples in panel A. The inset shows the FRET efficiency calculated from quenching of QD PL as a function of the number of Pep-A555 per QD. (C) The A555/QD PL ratio as a function of the number of Pep-A555 per QD averaged over three replicate experiments.

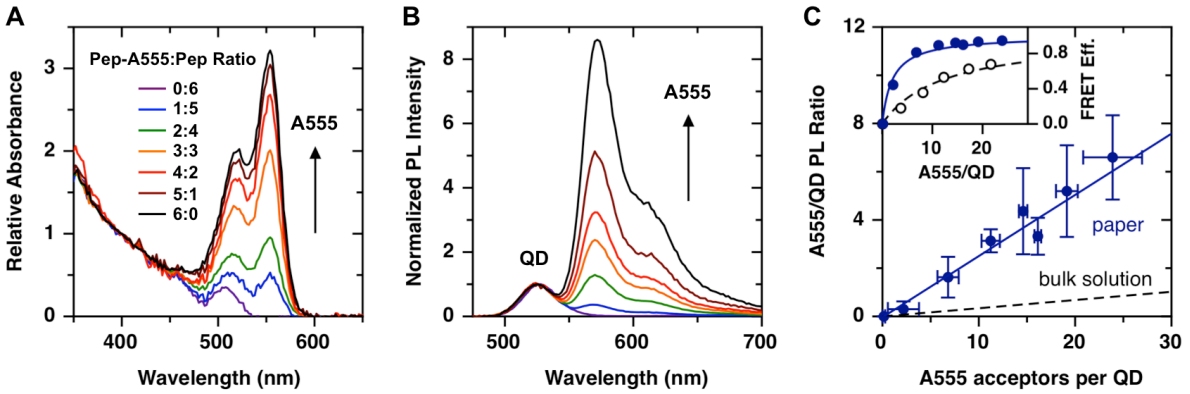

Fig. 7. Paper-phase FRET. (A) Representative absorption spectra showing the paper-phase assembly of increasing amounts of A555-labeled peptide per QD (from a 0:6 to 6:0 mixture of labeled and unlabeled peptide). The spectra are used to determine the actual number of Pep-A555 assembled per QD. (B) PL emission spectra corresponding to the samples in panel A. (C) The A555/QD PL ratio as a function of the number of Pep-A555 per QD averaged over three replicate experiments. The line-of-best-fit from the solution-phase data in Fig. 5C is shown for reference. The inset shows the FRET efficiency calculated from the ratio of QD and A555 PL as a function of the number of Pep-A555 per QD for both the solution-phase data (black open circles; data from Fig. 5B) and paper-phase data (blue closed circles; data from panel B, this figure).

absorption coefficients (~420 000 M^{-1} cm^{-1} for the QD at 506 nm; see Table 2 for A555). PL spectra showed a progressive decrease in QD PL and increase in sensitized A555 PL, which is characteristic of FRET (Fig. 5B). Analysis of the FRET efficiency from steady-state quenching (Fig. 5B, inset) indicated that the acceptor was situated ~7.1 nm away from the center of the QDs, or approximately 4 nm from the surface of the QD (~6 nm diameter). The A555/QD PL ratio increased linearly as the number of A555 acceptors per QD increased, as shown in Fig. 5C. A linear trend is expected for an ideal FRET pair with a fluorescent acceptor [39].

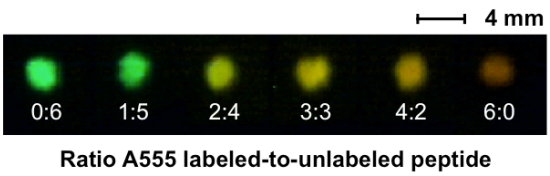

Fig. 6. Color digital camera image of spots of immobilized QDs on paper substrates assembled with different ratios of (an excess) of A555-labeled and unlabeled peptide. The green color is QD PL and the orange/red color is FRET-sensitized A555 PL. The image was taken under violet LED illumination (405 nm) with a long-pass filter (500 nm cutoff).

C. FRET on Paper Substrates

QDs were immobilized on paper substrates *via* **3b** and peptides were assembled on the QDs from solutions with different ratios of unlabeled and A555-labeled peptide. This method permitted variation of the number of acceptors per QD. Since the exact number of QDs retained in the paper matrix was unknown, the peptides could not be stoichiometrically self-assembled from solution. Instead, sufficient peptide was added to saturate the surface of the QDs so that the relative amount of A555-labeled peptide in solution would determine the number of acceptors per immobilized QD. A saturating quantity of peptide was also expected to minimize heterogeneity across the spot of immobilized QDs. Fig. 6 shows a color image, taken under violet LED light (405 nm), of spots of immobilized QDs on paper substrates with different ratios of labeled and unlabeled substrate. As the amount of labeled substrate increased, the color of the spots changed from green to yellow, indicating increasing quenching of QD PL and sensitization of A555 emission due to FRET.

Absorption and PL measurements were done on similarly prepared paper substrates to investigate FRET quantitatively.

Representative data is shown in Fig. 7A-B. The absorbance spectra appear much the same as those for QD-Pep-A555 conjugates in bulk solution; however, the PL spectra show much more intense A555 emission. Note that both the absorption and PL spectra are normalized to account for variations in absorbance and PL intensity between paper samples. These variations arise from the high scattering background of the paper, the uncertain path length through the paper, and different relative amounts of fiber volume and void space in different regions of interest. Normalization permitted determination of the relative number of Pep-A555 per QD and the corresponding A555/QD PL ratio. Fig. 7C shows the change in PL ratio as the number of A555 per QD increased on the paper substrates. The slope of the trend line through the data is > 7-fold larger than for bulk solution, suggesting a substantial enhancement in the ensemble rate of FRET.

The FRET efficiency was estimated from the relative QD and A555 PL intensities in Fig. 7B and is plotted in the inset of Fig. 7C. From this data, an *effective* QD-A555 separation of ~6.1 nm was calculated. An analogous calculation using the bulk solution PL spectra in Fig. 5B returns a value of ~8.2 nm. This value is somewhat larger than the 7.1 nm measured from only quenching of QD PL in solution, which is expected to be the more accurate value. Nonetheless, there is a clear enhancement of FRET.

D. Fluorescence Lifetime Imaging Microscopy

To further investigate the apparent enhancement of FRET within the paper matrix, FLIM measurements were done. This technique is ideal for this purpose since the time-domain PL data is relatively immune to differences in absolute steady-state intensity and background levels between samples. To provide the best possible comparison between bulk solution and the paper matrix, we switched from a two-step immobilization method to a one-step immobilization method with pre-assembled QD-peptide conjugates (see Materials and Methods). In this manner, precisely the same conjugates were measured between bulk solution and the paper matrix.

Fig. 8A-F shows fluorescence lifetime images for paper substrates modified with QD-Pep-A555 conjugates with nominal valences of 0, 4, 8, 16, and 20 labeled peptides per QD. The QDs in solution had an average lifetime of 5.5 ns whereas the immobilized QDs had a lifetime of 4.0 ns. In both bulk solution and paper formats, there is a clear decrease in the lifetime of the QDs as the number of A555 acceptors per QD increases. Lifetime distributions for the conjugates in bulk solution and immobilized in the paper matrix are shown in Fig. 8G-H. The FRET efficiencies for the two environments are calculated and compared in Fig. 8I. Once again, there is a clear enhancement of FRET efficiency for the paper samples. Analysis indicates that the *effective* donor-acceptor distance decreased from ~7.4 nm in bulk solution (*cf.* 7.1–8.2 from steady-state measurements) to ~6.3 nm in the paper matrix (*cf.* 6.1 nm from relative steady-state PL measurements). Further analysis indicated that the rate of FRET per acceptor (8) increased from 2.5 (± 0.9) × 10^7 s^{-1} in bulk solution to ~1.1 × 10^8 s^{-1} in the paper matrix. As before, the number of acceptors per QD was determined from absorbance measurements for both systems. While the measured and nominal values of acceptors per QD were in good agreement for the bulk solution samples, a negative deviation was observed for the analogous paper samples. This effect may be due to actual displacement of some bound peptide when QDs are immobilized on paper fibers or perhaps a change in the absorption properties of A555 within the paper matrix (although no spectral shifts in support of this hypothesis were observed). Nonetheless, even if the measurement of the number of A555 per QD has a small negative bias, the enhancement of FRET in the paper matrix remains substantial.

One possible reason for the enhancement in FRET in the paper matrix is a real change in the average distance between the QD donor and dye acceptor. This change could result from a change in the average conformation of the peptide bridge. However, between bulk solution and the paper matrix, the peptide remains bound to the same QDs under the same buffer conditions. Although possible, it is not clear that there should be a significant change in the interaction between the peptide, the interface of the QDs, or the solvated environment. Alternatively, enhanced FRET may be observed within the paper matrix because of the immobilization of multiple QD-Pep-A555 conjugates within close proximity to one another. The single donor-multiple acceptor systems in bulk solution could become a more complex multiple donor-multiple acceptor system with higher rates of FRET because of the greater overall number of donor-acceptor interactions. The QD-A555 separation values reported for the paper matrix are "effective" values because, in contrast to bulk solution, it is not clear that the immobilized QD-A555 assemblies can be treated as being centrosymmetric. Rather, there may be a distribution of donor-acceptor distances. Ongoing work is aimed at modeling these systems to better understand the source of the enhancement.

E. Proteolytic Assays

To demonstrate the bioanalytical utility of QD-peptide conjugates immobilized in a paper matrix, a model trypsin (TRP) inhibition assay was done. TRP is a serine protease that selectively cleaves peptide bonds C-terminal to arginine and lysine residues [81] and is critical in food digestion, cellular signaling, and even neurological processes [82]. In addition to being overactive in pancreatitis [83], TRP produced by tumor cells is thought to contribute to tumor growth and invasion [84]. TRP inhibitors are also important as, for example, pancreatic secretory TRP inhibitor (PSTI), also called tumor associated TRP inhibitor (TATI), is a marker for adverse prognosis in pancreatitis and kidney, bladder, and ovarian cancers [85].

Here, we assay the inhibitory action of aprotinin on TRP. Aprotinin is a well-known and potent inhibitor of TRP and many other serine proteases [86]. It has been used as a anti-fibrinolytic and anti-inflammatory agent during cardiac surgery [87]. Fig. 9A shows progress curves for the digestion of immobilized QD-Sub(TRP)-A555 conjugates over 20 min by 2 μM TRP in the presence of 0–40 μM aprotinin. The

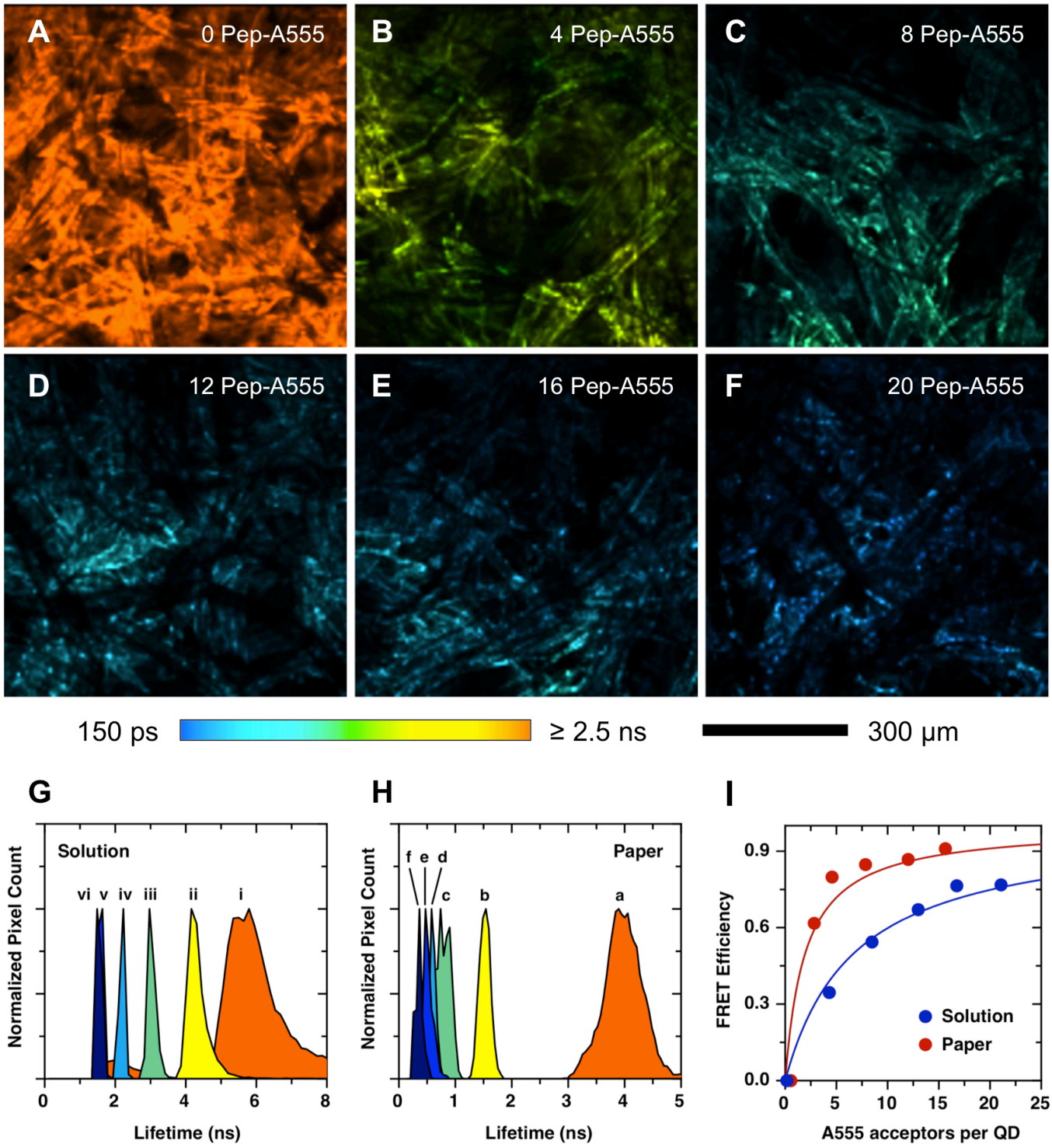

Fig. 8. Fluorescence lifetime images of paper substrates modified with pre-assembled QD-Pep-A555 conjugates at nominal valences of (A) 0, (B) 4, (C) 8, (D) 12, (E) 16, and (F) 20 A555 per QD. (G) Normalized fluorescence lifetime distributions for the six different conjugates in bulk solution: (i) 0, (ii) 4, (iii) 8, (iv) 12, (v) 16, and (vi) 20 A555 per QD. (H) Fluorescence lifetime distributions for the same conjugates subsequently immobilized on paper substrates. The lowercase letters correspond to the data in panels A-F. (I) Comparison of the FRET efficiency calculated from the decrease in QD PL lifetime between bulk solution (panel G) and the paper substrates (panel H).

normalized progress curves show progressively lower TRP activity as the concentration of aprotinin increases. Normalization of the FRET ratio to a control sample with no TRP accounts for non-proteolytic changes in the PL ratio over time and any small differences in initial FRET ratio between different spots or paper substrates. In Fig. 9B, a dose-response curve plotting the initial rate of change in normalized PL ratio *versus* aprotinin concentration shows a sharp transition between full activity and almost no activity. Such a sharp transition is expected given the high-affinity of aprotinin for

trypsin (K_d ~ 10^{-13} M) [88]. The IC50 value derived from Fig. 9B is 2.7 µM. The data demonstrate that paper substrates are a potential low-cost platform for assaying enzyme inhibitor potency for applications such as drug screening.

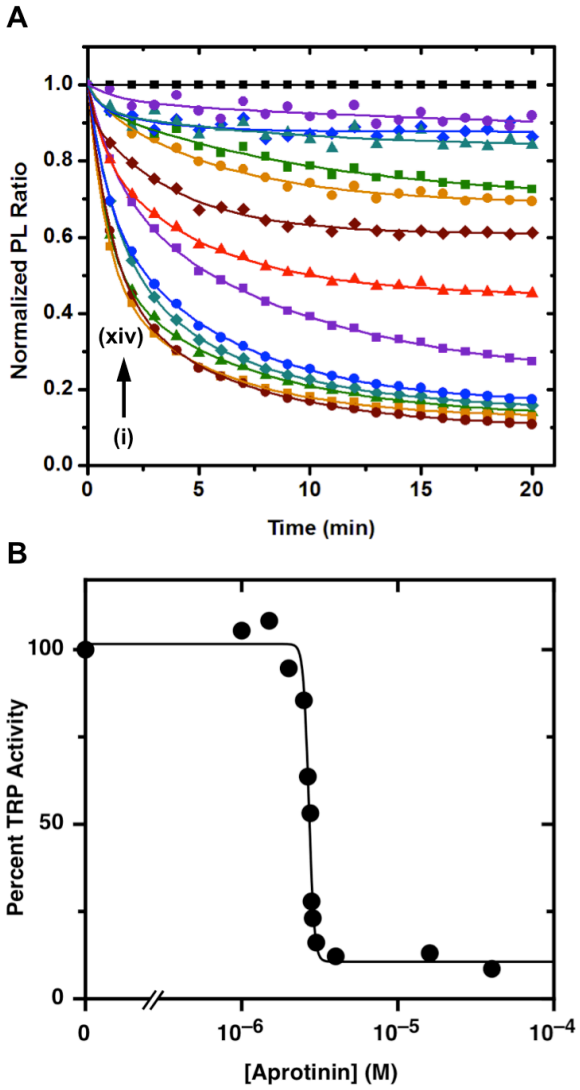

Fig 9. (A) Normalized progress curves for the digestion of paper-immobilized QD-Sub(TRP)-A555 conjugates by TRP (2 µM) in the presence of increasing amounts of aprotinin: (i) 0, (ii) 1.0, (iii) 1.5, (iv) 2.0, (v) 2.5, (vi) 2.65, (vii) 2.75, (viii) 2.8, (ix) 2.85, (x) 3.0, (xi) 4, (xii) 16, and (xiii) 40 µM. The curve (xiv) is a sample with no TRP that serves as a reference point for correcting data for non-proteolytic changes in PL signals and variations between different spots of QDs. The y-axis can be effectively read as the fraction of peptide substrate remaining. (B) Dose-response curve corresponding to the data in panel A. The activity was estimated from the initial rate of change in the normalized PL ratio.

V. Conclusion

In conclusion, we have (i) evaluated methods for the immobilization of QDs on cellulose paper fibers *via* self-assembly, (ii) identified enhancements in the rate and efficiency of FRET between immobilized QD donors and proximal dye acceptors within a paper matrix, and (iii) demonstrated the utility of such a system for assaying the inhibition of proteolytic activity. Both steady-state and time-resolved fluorescence analyses suggest a shorter effective donor-acceptor distance, resulting in an approximately 4-fold enhancement in the rate of FRET. This enhancement lends itself to assays where changes in the QD donor PL and FRET-sensitized acceptor dye PL are used to track or measure biomolecular activity. This capability was apparent in a semi-quantitative protease inhibition assay with TRP and aprotinin. Overall, the immobilization of QDs on paper substrates is a promising platform for new methods of bioanalysis.

References

[1] T. C. Dinadayalane and J. Leszczynski, "Remarkable diversity of carbon-carbon bonds: structures and properties of fullerenes, carbon nanotubes, and graphene," *Struct. Chem.,* vol. 21, pp. 1155-1169, 2010.

[2] V. N. Mochalin, O. Shenderova, D. Ho, and Y. Gogotsi, "The properties and applications of nanodiamonds," *Nat. Nanotechnol.,* vol. 7, pp. 11-13, 2012.

[3] E. C. Dreaden, A. M. Alkilany, X. H. Huang, C. J. Murphy, and M. A. El-Sayed, "The golden age: gold nanoparticles for biomedicine," *Chem. Soc. Rev.,* vol. 41, pp. 2740-2779, 2012.

[4] H. F. Qian, M. Z. Zhu, Z. K. Wu, and R. C. Jin, "Quantum Sized Gold Nanoclusters with Atomic Precision," *Acc. Chem. Res.,* vol. 45, pp. 1470-1479, 2012.

[5] F. Wang, D. Banerjee, Y. S. Liu, X. Y. Chen, and X. G. Liu, "Upconversion nanoparticles in biological labeling, imaging, and therapy," *Analyst,* vol. 135, pp. 1839-1854, 2010.

[6] W. R. Algar, K. Susumu, J. B. Delehanty, and I. L. Medintz, "Semiconductor Quantum Dots in Bioanalysis: Crossing the Valley of Death," *Anal. Chem.,* vol. 83, pp. 8826-8837, 2011.

[7] K. Boeneman, B. C. Mei, A. M. Dennis, G. Bao, J. R. Deschamps, H. Mattoussi, and I. L. Medintz, "Sensing Caspase 3 Activity with Quantum Dot-Fluorescent Protein Assemblies," *J. Am. Chem. Soc.,* vol. 131, pp. 3828-3829, 2009.

[8] C. Y. Zhang, H. C. Yeh, M. T. Kuroki, and T. H. Wang, "Single-quantum-dot-based DNA nanosensor," *Nat. Mater.,* vol. 4, pp. 826-831, 2005.

[9] R. Elghanian, J. J. Storhoff, R. C. Mucic, R. L. Letsinger, and C. A. Mirkin, "Selective Colorimetric Detection of Polynucleotides Based on the Distance-Dependent Optical Properties of Gold Nanoparticles," *Science,* vol. 277, pp. 1078-1081, 1997.

[10] C. Tassa, J. L. Duffner, T. A. Lewis, R. Weissleder, S. L. Schreiber, A. N. Koehler, and Y. S. Shaw, "Binding Affinity and Kinetic Analysis of Targeted Small Molecule-Modified Nanoparticles," *Bioconjugate Chem.,* vol. 21, pp. 14-19, 2010.

[11] W. R. Algar, A. Malonoski, J. R. Deschamps, J. B. Blanco-Canosa, K. Susumu, M. H. Stewart, B. J. Johnson, P. E. Dawson, and I. L. Medintz, "Proteolytic Activity at Quantum Dot-Conjugates: Kinetic Analysis Reveals Enhanced Enzyme Activity and Localized Interfacial "Hopping"," *Nano Lett.,* vol. 12, pp. 3793-3802, 2012.

[12] E. Petryayeva, W. R. Algar, and I. L. Medintz, "Quantum Dots in Bioanalysis: A Review of Applications Across Various Platforms for Fluorescence Spectroscopy and Imaging," *Appl. Spectrosc.,* vol. 67, pp. 215-252, 2013.

[13] E. J. Maxwell, A. D. Mazzeo, and G. M. Whitesides, "Paper-Based Electroanalytical Devices for Accessible Diagnostic Testing," *MRS Bulletin,* vol. 38, pp. 309-314, 2013.

[14] A. W. Martinez, S. T. Phillips, G. M. Whitesides, and E. Carrilho, "Diagnostics for the Developing World: Microfluidic Paper-Based Analytical Devices," *Anal. Chem.,* vol. 82, pp. 3-10, 2010.

[15] C. Sicard and J. D. Brennan, "Bioactive Paper: Biomolecule Immobilization Methods and Applications in Environmental Monitoring," *MRS Bulletin,* vol. 38, pp. 331-334, 2013.

[16] C. Parolo and A. Merkoci, "Paper-Based Nanobiosensors for Diagnostics," *Chem. Soc. Rev.,* vol. 42, pp. 450-457, 2013.

[17] A. H. Alhasan, D. Y. Kim, W. L. Daniel, E. Watson, J. J. Meeks, C. S. Thaxton, and C. A. Mirkin, "Scanometric MicroRNA Array Profiling of Prostate Cancer Markers Using Spherical Nucleic

Acid-Gold Nanoparticle Conjugates," *Anal. Chem.,* vol. 84, pp. 4153-4160, 2012.

[18] Z. H. Li, Y. Wang, J. Wang, Z. W. Tang, J. G. Pounds, and Y. H. Lin, "Rapid and Sensitive Detection of Protein Biomarker Using a Portable Fluorescence Biosensor Based on Quantum Dots and a Lateral Flow Test Strip," *Anal. Chem.,* vol. 82, pp. 7008-7014, 2010.

[19] A. N. Berlina, N. A. Taranova, A. V. Zherdev, Y. Y. Vengerov, and B. B. Dzantiev, "Quantum dot-based lateral flow immunoassay for detection of chloramphenicol in milk," *Anal. Bioanal. Chem.,* vol. 405, pp. 4997-5000, 2013.

[20] Z. X. Zou, D. Du, J. Wang, J. N. Smith, C. Timchalk, Y. Q. Li, and Y. H. Lin, "Quantum Dot-Based Immunochromatographic Fluorescent Biosensor for Biomonitoring Trichloropyridinol, a Biomarker of Exposure to Chlorpyrifos," *Anal. Chem.,* vol. 82, pp. 5125-5133, 2010.

[21] M. O. Noor, A. Shahmuradyan, and U. J. Krull, "Paper-Based Solid-Phase Nucleic Acid Hybridization Assay Using Immobilized Quantum Dots as Donors in Fluorescence Resonance Energy Transfer," *Anal. Chem.,* vol. 85, pp. 1860-1867, 2013.

[22] J. P. Yuan, N. Gaponik, and A. Eychmuller, "Application of Polymer Quantum Dot-Enzyme Hybrids in the Biosensor Development and Test Paper Fabrication," *Anal. Chem.,* vol. 84, pp. 5047-5052, 2012.

[23] P. Zrazhevskiy, M. Sena, and X. H. Gao, "Designing multifunctional quantum dots for bioimaging, detection, and drug delivery," *Chem. Soc. Rev.,* vol. 39, pp. 4326-4354, 2010.

[24] S. J. Rosenthal, J. C. Chang, O. Kovtun, J. R. McBride, and I. D. Tomlinson, "Biocompatible quantum dots for biological applications," *Chem. Biol.,* vol. 18, pp. 10-24, 2011.

[25] U. Resch-Genger, M. Grabolle, S. Cavaliere-Jaricot, R. Nitschke, and T. Nann, "Quantum dots versus organic dyes and fluorescent labels," *Nat. Methods,* vol. 5, pp. 763-775, 2008.

[26] W. R. Algar, A. J. Tavares, and U. J. Krull, "Beyond labels: A review of the application of quantum dots as integrated components of assays, bioprobes, and biosensors utilizing optical transduction," *Anal. Chim. Acta,* vol. 673, pp. 1-25, 2010.

[27] I. L. Medintz and H. Mattoussi, "Quantum dot-based resonance energy transfer and its growing application in biology," *Phys. Chem. Chem. Phys.,* vol. 11, pp. 17-45, 2009.

[28] J. H. Kim, D. Morikis, and M. Ozkan, "Adaptation of inorganic quantum dots for stable molecular beacons," *Sens. Actuators B,* vol. 102, pp. 315-319, 2004.

[29] I. L. Medintz, A. R. Clapp, F. M. Brunel, T. Tiefenbrunn, H. T. Uyeda, E. L. Chang, J. R. Deschamps, P. E. Dawson, and H. Mattoussi, "Proteolytic activity monitored by fluorescence resonance energy trransfer through quantum-dot-peptide conjugates," *Nat. Mater.,* vol. 5, pp. 581-589, 2006.

[30] K. Boeneman, D. E. Prasuhn, J. B. Blanco-Canosa, P. E. Dawson, J. S. Melinger, M. Ancona, M. H. Stewart, K. Susumu, A. Huston, and I. L. Medintz, "Self-Assembled Quantum Dot-Sensitized Multivalent DNA Photonic Wires," *J. Am. Chem. Soc.,* vol. 132, pp. 18177-18190, 2010.

[31] H. Lu, O. Schöps, U. Woggon, and C. M. Niemeyer, "Self-assembled donor comprising quantum dots and fluorescent proteins for long-range fluorescence resonance energy transfer," *J. Am. Chem. Soc.,* vol. 130, pp. 4815-4827, 2008.

[32] I. L. Medintz, T. Pons, K. Susumu, K. Boeneman, A. M. Dennis, D. Farrell, J. R. Deschamps, J. S. Melinger, G. Bao, and H. Mattoussi, "Resonance Energy Transfer Between Luminescent Quantum Dots and Diverse Fluorescent Protein Acceptors," *J. Phys. Chem. C,* vol. 43, pp. 18552-18561, 2009.

[33] T. Pons, I. L. Medintz, K. E. Sapsford, S. Higashiya, A. F. Grimes, D. S. English, and H. Mattoussi, "On the quenching of semicondutor quantum dot photoluminescence by proximal gold nanoparticles," *Nano Lett.,* vol. 7, pp. 3157-3164, 2007.

[34] Y. P. Kim, Y. H. Oh, E. Oh, S. Ko, M. K. Han, and H. S. Kim, "Energy Transfer-Based Multiplexed Assay of Proteases by Using Gold Nanoparticle and Quantum Dot Conjugates on a Surface," *Anal. Chem.,* vol. 80, pp. 4634-4641, 2008.

[35] E. Morales-Narváez, B. Pérez-López, L. B. Pires, and A. Merkoçi, "Simple Förster resonance energy transfer evidence for the ultrahigh quantum dot quenching efficiency by graphene oxide compared to other carbon structures " *Carbon,* vol. 50, pp. 2987-2993, 2012.

[36] E. Shafran, B. D. Mangum, and J. M. Gerton, "Energy Tranfer From an Individual Quantum Dot to a Carbon Nanotube," *Nano Lett.,* vol. 10, pp. 4049-4054, 2010.

[37] M. Liu, H. Zhao, X. Quan, S. Chen, and X. Fan, "Distance-independent quenching of quantum dots by nanoscale-graphene in self-assembled sandwich immunoassay," *Chem. Commun.,* vol. 46, pp. 7909-7911, 2010.

[38] D. Geißler, L. J. Charbonnière, R. F. Ziessel, N. G. Butlin, H.-G. Löhmannsröben, and N. Hildebrandt, "Quantum Dot Biosensors for Ultrasensitive Multiplexed Diagnostics," *Angew. Chem. Int. Ed.,* vol. 49, pp. 1396-1401, 2010.

[39] W. R. Algar, A. P. Malanoski, K. Susumu, M. H. Stewart, N. Hildebrandt, and I. L. Medintz, "Multiplexed Tracking of Protease Activity Using a Single Color of Quantum Dot Vector and a Time-Gated Förster Resonance Energy Transfer Relay," *Anal. Chem.,* vol. 84, pp. 10136-10146, 2012.

[40] R. Freeman and I. Willner, "Optical molecular sensing with semiconductor quantum dots (QDs)," *Chem. Soc. Rev.,* vol. 41, pp. 4067-4085, 2012.

[41] Z. Y. Xia and J. H. Rao, "Biosensing and imaging based on bioluminescence resonance energy transfer," *Curr. Opin. Biotechnol.,* vol. 20, pp. 37-44, 2009.

[42] Q. Wei, M. Lee, X. Yu, E. K. Lee, G. H. Seong, J. Choo, and Y. W. Cho, "Development of an open sandwich fluoroimmunoassay based on fluorescence resonance energy transfer," *Anal. Biochem.,* vol. 358, pp. 31-37, 2006.

[43] R. Gill, I. Willner, I. Shweky, and U. Banin, "Fluorescence Resonance Energy Transfer in CdSe/ZnS−DNA Conjugates: Probing Hybridization and DNA Cleavage," *J. Phys. Chem. B,* vol. 109, pp. 23715-23719, 2005.

[44] I. L. Medintz, A. R. Clapp, H. Mattoussi, E. R. Goldman, B. Fisher, and J. M. Mauro, "Self-assembled nanoscale biosensors based on quantum dot FRET donors," *Nat. Mater.,* vol. 2, pp. 630-638, 2003.

[45] C. H. Vannoy, L. Chong, C. Le, and U. J. Krull, "A competitive displacement assay with quantum dots as fluorescence resonance energy transfer donors," *Anal. Chim. Acta,* vol. 759, pp. 92-99, 2013.

[46] K. A. Cissell, S. Campbell, and S. K. Deo, "Rapid, single-step nucleic acid detection," *Anal. Bioanal. Chem.,* vol. 391, pp. 2577-2581, 2008.

[47] I. L. Medintz, L. Berti, T. Pons, A. F. Grimes, D. S. English, A. Alessandrini, P. Facci, and H. Mattoussi, "A reactive peptidic linker for self-assembling hybrid quantum dot-DNA bioconjugates," *Nano Lett.,* vol. 7, pp. 1741-1748, 2007.

[48] R. C. Somers, R. M. Lanning, P. T. Snee, A. B. Greytak, R. K. Jain, M. G. Bawendi, and D. G. Nocera, "A nanocrystal-based ratiometric pH sensor for natural pH ranges," *Chem. Sci.,* vol. 3, pp. 2980-2985, 2012.

[49] I. L. Medintz, A. R. Clapp, J. S. Melinger, J. R. Deschamps, and H. Mattoussi, "A reagentless biosensing assembly based on quantum dot-donor Förster resonance energy tranfser," *Adv. Mater.,* vol. 17, pp. 2450-2455, 2005.

[50] E. J. McLaurin, A. B. Greytak, M. G. Bawendi, and D. G. Nocera, "Two-Photon Absorbing Nanocrystal Sensor for Ratiometric Detection of Oxygen," *J. Am. Chem. Soc.,* vol. 131, pp. 12994-13001, 2009.

[51] R. Freeman, L. Bahshi, T. Finder, R. Gill, and I. Willner, "Competitive analysis of saccharides or dopamine by boronic acid-functionalized CdSe-ZnS quantum dots," *Chem. Commun.,* vol. 7, pp. 764-766, 2009.

[52] C. Y. Zhang and L. W. Johnson, "Single Quantum-Dot-Based Aptameric Nanosensor for Cocaine," *Anal. Chem.,* vol. 81, pp. 3051-3055, 2009.

[53] R. Freeman, T. Finder, R. Gill, and I. Willner, "Probing Protein Kinase (CK2) and Alkaline Phosphatase with CdSe/ZnS Quantum Dots," *Nano Lett.,* vol. 10, pp. 2192-1296, 2010.

[54] J. E. Ghadiali, B. E. Cohen, and M. M. Stevens, "Protein Kinase-Actuated Resonance Energy Transfer in Quantum Dot-Peptide Conjugates," *ACS Nano,* vol. 4, pp. 4915-4919, 2010.

[55] M. Xue, X. Wang, L. Duan, W. Gao, L. Ji, and B. Tang, "A new nanoprobe based on FRET between functional quantum dots and gold nanoparticles for fluoride anion and its applications for biological imaging," *Biosens. Bioelectron.,* vol. 36, pp. 168-173, 2012.

[56] B. Liu, F. Zeng, G. Wu, and S. Wu, "Nanoparticles as scaffolds for FRET-based ratiometric detection of mercury ions in water with QDs as donors," *Analyst,* vol. 137, pp. 3717-3724, 2012.

[57] Y. Long, L. F. Zhang, Y. Zhang, and C. Y. Zhang, "Single Quantum Dot Based Nanosensor for Renin Assay," *Anal. Chem.,* vol. 84, pp. 8846-8852, 2012.

[58] J. Qian, C. Wang, X. Pan, and S. Liu, "A high-throughput homogeneous immunoassay based on Förster resonance energy transfer between quantum dots and gold nanoparticles," *Anal. Chim. Acta,* vol. 763, pp. 43-49, 2013.

[59] S. Shin, H. Y. Nam, E. J. Lee, W. Jung, and S. S. Hah, "Molecular beacon-based quantitation of epithelial tumor marker mucin 1," *Bioorg. Med. Chem. Lett.,* vol. 22, pp. 6081-6084, 2012.

[60] W. R. Algar and U. J. Krull, "Toward A Multiplexed Solid-Phase Nucleic Acid Hybridization Assay Using Quantum Dots as Donors in Fluorescence Resonance Energy Transfer," *Anal. Chem.,* vol. 81, pp. 4113-4120, 2009.

[61] E. Petryayeva, W. R. Algar, and U. J. Krull, "Adapting Fluorescence Resonance Energy Transfer with Quantum Dot Donors for Solid-Phase Hybridization Assays in Microtiter Plate Format," *Langmuir,* vol. 29, pp. 977-987, 2013.

[62] W. R. Algar, M. G. Ancona, A. P. Malanoski, K. Susumu, and I. L. Medintz, "Assembly of a Concentric Förster Resonance Energy Transfer Relay on a Quantum Dot Scaffold: Characterization and Application to Multiplexed Protease Sensing," *ACS Nano,* vol. 6, pp. 11044-11058, 2012.

[63] J. R. Lakowicz, *Principles of Fluorescence Spectroscopy*, 3rd ed. New York: Springer, 2006.

[64] R. Pelton, "Bioactive Paper Provides a Low-Cost Platform for Diagnostics," *Trends Anal. Chem.,* vol. 28, pp. 925-942, 2009.

[65] K. Boeneman, J. R. Deschamps, J. B. Delehanty, K. Susumu, M. H. Stewart, R. H. Glaven, G. P. Anderson, E. R. Goldman, A. L. Huston, and I. L. Medintz, "Optimizing Protein Coordination to Quantum Dots with Designer Peptidyl Linkers," *Bioconjugate Chem.,* vol. 24, pp. 269-281, 2013.

[66] I. L. Medintz, J. H. Konnert, A. R. Clapp, I. Stanish, M. E. Twigg, H. Mattoussi, J. M. Mauro, and J. R. Deschamps, "A fluorescence resonance energy transfer-derived structure of a quantum dot-protein bioconjugate nanoassembly," *Proc. Natl. Acad. Sci. USA,* vol. 101, pp. 9612-9617, 2004.

[67] I. L. Medintz, T. Pons, J. B. Delehanty, K. Susumu, F. M. Brunel, P. E. Dawson, and H. Mattoussi, "Intracellular delivery of quantum dot-protein cargos mediated by cell penetrating peptides," *Bioconjugate Chem.,* vol. 19, pp. 1785-1795, 2008.

[68] D. E. Prasuhn, J. R. Deschamps, K. Susumu, M. H. Stewart, K. Boeneman, J. B. Blanco-Canosa, P. E. Dawson, and I. L. Medintz, "Polyvalent Display and Packing of Peptides and Proteins on Semiconductor Quantum Dots: Predicted Versus Experimental Results," *Small,* vol. 6, pp. 555-564, 2010.

[69] J. B. Delehanty, I. L. Medintz, T. Pons, F. M. Brunel, P. E. Dawson, and H. Mattoussi, "Self-assembled quantum dot-peptide bioconjugates for selective intracellular delivery," *Bioconjugate Chem.,* vol. 17, pp. 920-927, 2006.

[70] D. E. Prasuhn, J. B. Blanco-Canosa, G. J. Vora, J. B. Delehanty, K. Susumu, B. C. Mei, P. E. Dawson, and I. L. Medintz, "Combining Chemoselective Ligation with Polyhistidine-Driven Self-Assembly for the Modular Display of Biomolecules on Quantum Dots," *ACS Nano,* vol. 4, pp. 267-278, 2010.

[71] K. E. Sapsford, T. Pons, I. L. Medintz, S. Higashiya, F. M. Brunel, P. E. Dawson, and H. Mattoussi, "Kinetics of Metal-Affinity Driven Self-Assembly between Proteins or Peptides and CdSe-ZnS Quantum Dots," *J. Phys. Chem. C,* vol. 111, pp. 11528-11538, 2007.

[72] K. Boeneman, J. R. Deschamps, S. Buckhout-White, D. E. Prashun, J. B. Blanco-Canosa, P. E. Dawson, M. H. Stewart, K. Susumu, E. R. Goldman, M. Ancona, and I. L. Medintz, "Quantum Dot DNA Bioconjugates: Attachment Chemistry Strongly Influences the Resulting Composite Architecture," *ACS Nano,* vol. 4, pp. 7253-7266, 2010.

[73] J. Wang and J. Xia, "Preferential Binding of a Novel Polyhistidine Peptide Dendrimer Ligand on Quantum Dots Probed by Capillary Electrophoresis," *Anal. Chem.,* vol. 83, pp. 6323-6329, 2011.

[74] A. M. Dennis, D. C. Sotto, B. C. Mei, I. L. Medintz, H. Mattoussi, and G. Bao, "Surface Ligand Effects on Metal-Affinity Coordination to Quantum Dots: Implications for Nanoprobe Self-Assembly," *Bioconjugate Chem.,* vol. 21, pp. 1160-1170, 2010.

[75] A. Dif, F. Boulmedais, M. Pinot, V. Roullier, M. Baudy-Floc'h, F. M. Coquelle, S. Clarke, P. Neveu, F. Vignaux, R. L. Borgne, M. Dahan, Z. Gueroui, and V. Marchi-Artzner, "Small and Stable Peptidic PEGylated Quantum Dots to Target Polyhistidine-Tagged Proteins with Controlled Stoichiometry," *J. Am. Chem. Soc.,* vol. 131, pp. 14738-14746, 2009.

[76] I. L. Medintz, K. E. Sapsford, A. R. Clapp, T. Pons, S. Higashiya, J. T. Welch, and H. Mattoussi, "Designer Variable Repeat Length Polypeptides as Scaffolds for Surface Immobilization of Quantum Dots," *J. Phys. Chem. B,* vol. 110, pp. 10683-10690, 2006.

[77] Y. Zhang and A. Clapp, "Overview of Stabilizing Ligands for Biocompatible Quantum Dot Nanocrystals," *Sensors,* vol. 11, pp. 11036-11055, 2011.

[78] B. C. Mei, K. Susumu, I. L. Medintz, J. B. Delehanty, T. J. Mountziaris, and H. Mattoussi, "Modular poly(ethylene glycol) ligands for biocompatible semiconductor and gold nanocrystals with extended pH and ionic stability," *J. Mater. Chem.,* vol. 18, pp. 4949-4958, 2008.

[79] K. Susumu, E. Oh, J. B. Delehanty, J. B. Blanco-Canosa, B. J. Johnson, V. Jain, W. J. Hervey, W. R. Algar, K. Boeneman, P. E. Dawson, and I. L. Medintz, "Multifunctional Compact Zwitterionic Ligands for Preparing Robust Biocompatible Semiconductor Quantum Dots and Gold Nanoparticles," *J. Am. Chem. Soc.,* vol. 133, pp. 9480-9496, 2011.

[80] W. R. Algar and U. J. Krull, "Interfacial Chemistry and the Design of Solid-Phase Nucleic Acid Hybridization Assays Using Immobilized Quantum Dots as Donors in Fluorescence Resonance Energy Transfer," *Sensors,* vol. 11, pp. 6214-6236, 2011.

[81] J. V. Olsen, S. E. Ong, and M. Mann, "Trypsin cleaves exclusively C-terminal to arginine and lysine residues," *Mol. Cell. Proteomics,* vol. 3, pp. 608-614, 2004.

[82] Y. Wang, W. Luo, and G. Reiser, "Trypsin and trypsin-like proteases in the brain: Proteolysis and cellular functions," *Cell. Mol. Life Sci.,* vol. 65, pp. 237-252, 2008.

[83] W. Halangk, M. M. Lerch, B. Brandt-Nedelev, W. Roth, M. Ruthenbuerger, T. Reinheckel, W. Domschke, H. Lippert, C. Peters, and J. Deussing, "Role of cathepsin B in intracellular trypsinogen activation and the onset of acute pancreatitis," *J. Clin. Invest.,* vol. 106, pp. 773-781, 2000.

[84] H. Yamamoto, S. Iku, Y. Adachi, A. Imsumran, H. Taniguchi, K. Nosho, Y. Min, S. Horiuchi, M. Yoshida, F. Itoh, and K. Imai, "Association of trypsin expression with tumour progression and matrilysin expression in human colorectal cancer," *J. Pathol.,* vol. 199, pp. 176-184, 2003.

[85] U. H. Stenman, "Tumor-associated Trypsin Inhibitor," *Clin. Chem.,* vol. 48, pp. 1206-1209, 2002.

[86] D. Pintigny and J. Dachary-Prigent, "Aprotinin can inhibit the proteolytic activity of thrombin," *Eur. J. Biochem.,* vol. 207, pp. 89-95, 1992.

[87] K. Martin, G. Wiesner, T. Breuer, R. Lange, and P. Tassani, "The Risks of Aprotinin and Tranexamic Acid in Cardiac Surgery: A One-Year Follow-Up of 1188 Consecutive Patients," *Anesthesia & Analgesia,* vol. 107, pp. 1783-1790, 2008.

[88] H. Fritz and G. Wunderer, "Biochemistry and Applications of Aprotinin, the Kallikrein Inhibitor from Bovine Organs," *Drug Res.,* vol. 33, pp. 479-494, 1983.

Hyungki Kim is currently pursuing a B.Sc. degree in chemistry at the University of British Columbia, Canada.

He is presently a research assistant and his current interests include developing chemosensors and biosensors on paper platforms.

Mr. Kim is a recipient of an NSERC Undergraduate Summer Research Award in 2013.

Eleonora Petryayeva received B.Sc. (2011) and M.Sc. (2012) degrees in chemistry from the University of Toronto, Canada.

She is currently pursuing a Ph.D. degree in bioanalytical

chemistry at the University of British Columbia, Canada. Her major research interests include the development of bioassays and biosensors using the unique optical properties of nanomaterials.

Ms. Petryayeva is a recipient of a prestigious NSERC Canada Graduate Scholarship.

W. Russ Algar received B.Sc. (2005), M.Sc. (2006), and Ph.D. (2010) degrees in chemistry from the University of Toronto, Canada.

He was a postdoctoral researcher at George Mason University and the Center for Bio/Molecular Science and Engineering, U.S. Naval Research Laboratory from 2010–2012. He is currently an assistant professor and a Canada Research Chair (Tier 2) in Chemical Sensing at the University of British Columbia, Canada. His research interests include developing nanoparticle probes and biosensors for point-of-care diagnostics and cellular sensing, investigating novel energy transfer configurations based on nanomaterials, and understanding the nano-bio interface.

Dr. Algar has received 13 research awards and fellowships since 2005.